

HOPE: A Reinforcement Learning-based Hybrid Policy Path Planner for Diverse Parking Scenarios

Mingyang Jiang, Yueyuan Li, Songan Zhang, Chunxiang Wang, and Ming Yang

Abstract—Path planning plays a pivotal role in automated parking, yet current methods struggle to efficiently handle the intricate and diverse parking scenarios. One potential solution is the reinforcement learning-based method, leveraging its exploration in unrecorded situations. However, a key challenge lies in training reinforcement learning methods is the inherent randomness in converging to a feasible policy. This paper introduces a novel solution, the Hybrid Policy Path planner (HOPE), which integrates a reinforcement learning agent with Reeds-Shepp curves, enabling effective planning across diverse scenarios. The paper presents a method to calculate and implement an action mask mechanism in path planning, significantly boosting the efficiency and effectiveness of reinforcement learning training. A transformer is employed as the network structure to fuse environmental information and generate planned paths. To facilitate the training and evaluation of the proposed planner, we propose a criterion for categorizing the difficulty level of parking scenarios based on space and obstacle distribution. Experimental results demonstrate that our approach outperforms typical rule-based algorithms and traditional reinforcement learning methods, showcasing higher planning success rates and generalization across various scenarios. The code for our solution will be openly available on <https://github.com/jiamiya/HOPE>.

Index Terms—Automated parking, reinforcement learning, path planning.

I. INTRODUCTION

Automatic parking technology has gained attention in recent years due to its potential benefits in safety and time efficiency [1]. The entire automated parking systems comprise several vital components, including perception, planning, and control, among which path-planning algorithms play a crucial role [2]. The path-planning task in parking scenarios involves generating a feasible path that links the vehicle’s start position and the target position in the parking spots, as well as considering the vehicle’s physics constraints. While existing rule-based path-planning approaches prove practical and robust in most simple scenarios, their inherent difficulty in truly understanding the surrounding environment may lead to planning failures, especially when scenarios become more intricate [3].

Learning-based planners have the potential to understand environments and intelligently plan routes through a data-

driven approach, diverging from reliance on pre-defined planning methods rooted in human priors. While in various tasks, expert data is used as the ground truth for imitation learning, the scarcity of large-scale datasets for parking scenarios necessitates researchers to collect data manually [4]. This supervised learning approach poses the risk of overfitting the model to specific parking strategies due to the insufficient diversity in the training scenarios. Meanwhile, reinforcement learning has gathered increasing attention in the field of autonomous driving [5]. Indeed, through interaction with the environment, reinforcement learning enables the training of intelligent planners without the need for labeled trajectory ground truth. Nonetheless, training reinforcement learning agents in complex and diverse scenarios remains a challenging task [6]. It is straightforward for the agent to fit into fixed parking strategies but poses greater difficulty in obtaining generalization capability across various parking scenarios. Moreover, the agent faces challenges in conducting effective exploration, especially in complex scenarios with narrow parking spaces, which significantly impacts training efficiency.

This paper focuses on employing reinforcement learning methods in the parking path planning task with static obstacles. To achieve efficient and effective learning under diverse parking scenarios, we propose reinforcement learning-based Hybrid Policy Path planner (HOPE). The hybrid policy planner is designed to leverage the reinforcement learning-based actor-critic method and a classical geometric-based method, the Reeds-Shepp (RS) curve [7]. A transformer-based structure is used as the information fusion network in actor and critic networks [8]. Meanwhile, since the diversity of scenario difficulty has a significant impact on training and testing, we rank the difficulty of scenarios by referencing related standards for automated parking. Overall, the main contributions of this paper include:

- We develop a hybrid policy method for parking path planning, which takes advantage of both learning-based and rule-based methods to achieve generalization capability under diverse parking scenarios.
- We propose a method for calculating and implementing the action mask in the path planning task. This mechanism excludes improper actions for reinforcement learning agents and significantly improves training efficiency and performance.
- We propose a criterion to rank the difficulty of static parking scenarios. Comprehensive experiments are conducted across simulations of different difficulty levels, demonstrating a notable improvement in success rates

This work is supported in part by the National Natural Science Foundation of China under Grants 62173228 (Corresponding author: Ming Yang and Yueyuan Li).

Mingyang Jiang, Yueyuan Li, Chunxiang Wang, and Ming Yang are with the Department of Automation, Shanghai Jiao Tong University, Key Laboratory of System Control and Information Processing, Ministry of Education of China, Shanghai, 200240, CN (email: MingYANG@sjtu.edu.cn, rowena_lee@sjtu.edu.cn).

Songan Zhang is with the Global Institute of Future Technology, Shanghai Jiao Tong University, Shanghai, 200240, CN

compared to rule-based and naive reinforcement learning-based methods.

II. RELATED WORK

A. Non-learning-based parking path-planning

Non-learning-based path planning methods under parking scenarios mainly include geometric-based methods and sampling-and-search-based methods [9]. Geometric planners construct paths connecting the start position and the target position using different kinds of geometric curves [10, 11]. The most classic geometric methods include the Dubins curves and the RS curves [7, 12]. Building upon the RS curve, several improvements have been made to enhance its performance in parking scenarios [13, 14]. The sampling-and-search-based approach discretizes and searches either in the state space or in the control space to find a valid path. One widely employed approach is the Hybrid A* method [15], which devises a variant of the A* algorithm that incorporates the kinematic state space of the vehicle to derive a kinematically feasible trajectory. Hybrid A* was initially utilized in the Defense Advanced Research Projects Agency Challenge (DARPA) and has since undergone improvements and application to path planning tasks in parking scenarios [16, 17]. Both geometric and sampling-and-search-based methods, as rule-based methods, leverage human prior knowledge to design algorithms. In most common cases, these priors can serve as a strong fallback to obtain satisfactory solutions. However, it remains challenging for rule-based methods to achieve human-level proficiency in complex and diverse parking scenarios [18].

Another category of methods involving path planning is the optimization-based trajectory planning approach. These methods solve the trajectory planning problem by formulating it as an optimal control problem. Related works have made improvements in collision avoidance constraint formulation [19], iterative solution efficiency [9], and robustness [20]. While this approach can yield smoother paths that adhere to vehicle kinematics compared to rule-based path-planning algorithms, the optimization process relies on another path-planning algorithm, often the Hybrid A* method [19–21], to obtain initial solutions. Therefore, these methods are typically used in conjunction with path planning algorithms to generate smoother trajectories rather than being employed independently for feasible path generation.

B. Learning-based parking path-planning

Learning-based methods represent a potential avenue to enhance the planner's performance in the task of parking. Existing methods mainly include imitating learning-based and reinforcement learning-based methods. Imitating learning requires the learnable planner to fit on the ground truth data. Liu et al. employed a neural network to align parking paths more closely with human behavior [22]. Rathour S et al. derived a parking policy by imitating trajectories collected from expert drivers [23]. Other works include implementing the deep neural network or deep recurrent neural network on real vehicles [24, 25]. However, existing imitation learning-based approaches still lack diversity and complexity in scenarios, and

the behavior cloners cannot surpass the performance of their imitation targets [26].

In the reinforcement learning-based approaches, intelligent planners can be obtained without the labeled ground truth by interacting with the environment. The Monte Carlo tree search method was applied to search the available path in parallel parking scenarios [27]. Bernhard J et al. learned the heuristics with Deep Q-learning (DQL) and improved the path search process in the Hybrid A* algorithm [28, 29]. Du et al. directly employed DQL to train an agent to produce single-step path planning results iteratively in a parallel and vertical case [30]. Yuan et al. proposed a hierarchical planning approach where high-level reinforcement learning agents are trained to generate initial reference solutions [31]. The existing works typically map the elements of the task to the components of reinforcement learning and directly employ them to train the agent in a limited number of scenarios. As more complex and diverse parking scenarios are introduced, it would be harder for reinforcement learning-based methods to explore the proper parking policy, making it challenging to obtain planners with generalization capabilities.

III. PRELIMINARIES

A. Reinforcement learning for path planning

The reinforcement learning problem can be addressed as policy learning in a Markov decision process (MDP) defined by a 4-element tuple $(\mathcal{S}, \mathcal{A}, p, r)$, where \mathcal{S} is the state space, and \mathcal{A} is the action space. In the path-planning problem, $s_t \in \mathcal{S}$ includes the vehicle position and orientation $p_t = (x_t, y_t, \theta_t)$ as well as other observable information about obstacles and target parking space. We select velocity v and steering angle δ as the action space $\mathcal{A} = \{a = (v, \delta)\}$. p denotes the state transition probability density of the next state s_{t+1} given the current state s_t and action a_t . In practice, the transition is modeled using the single-track bicycle model, as implemented in [32], and this uncertainty is not considered in a deterministic environment. A reward $r = r(s_{t+1}, a_t)$ is given by the environment E based on the state and action in each step. The objective is to learn the policy $\pi(a_t|s_t)$ that maximizes the future reward $R_t = \sum_{i=t}^T \gamma^{(i-t)} r(s_i, a_i)$ with a discounting factor $\gamma \in [0, 1]$. Given the start point p_0 and the target p_T , the feasible parking path $P = \{p_0, p_1, p_2, \dots, p_T\}$ can be obtained iteratively using the policy π .

To obtain the optimal policy, reinforcement learning algorithms primarily use the action-value function to describe the reward in terms of expectation after taking action a_t in state s_t with policy π :

$$\begin{aligned} Q_\pi(s_t, a_t) &= E_{i>t, s_i \sim E, a_i \sim \pi} [R_t | s_t, a_t] \\ V_\pi(s_t) &= E_{a_t \sim \pi(\cdot | s_t)} [Q_\pi(s_t, a_t)], \end{aligned} \quad (1)$$

and both the Q function and value function can be updated by the Bellman equation:

$$\begin{aligned} Q_\pi(s_t, a_t) &= E_{r_t, s_{t+1} \sim E} [r(s_t, a_t) + \gamma Q_\pi(s_{t+1}, a_{t+1})] \\ V_\pi(s_t) &= E_{a_t \sim \pi(\cdot | s_t)} [r(s_t, a_t) + \gamma V_\pi(s_{t+1})]. \end{aligned} \quad (2)$$

To demonstrate the improvement of our proposed method across different reinforcement learning approaches, in this

paper, we chose the commonly used on-policy algorithm, Proximal Policy Gradient (PPO) [33], and off-policy algorithm, Soft Actor-Critic (SAC) [34], to obtain the reinforcement learning policy π_θ in HOPE.

1) *PPO*: PPO is a policy-gradient method that performs the gradient ascent in the trust region. To model the change between the old policy parameters $\pi_{\theta_{old}}$ before the update and the new parameters π_θ , a probability ratio is denoted as $r_t(\theta) = \frac{\pi_\theta(a_t|s_t)}{\pi_{\theta_{old}}(a_t|s_t)}$. The loss function is:

$$L(\theta) = \hat{E}_t \left[\min \left(r_t(\theta) \hat{A}_t, \text{clip}(r_t(\theta), 1 - \epsilon, 1 + \epsilon) \hat{A}_t \right) \right] \quad (3)$$

where $\hat{A}_t = Q(s_t, a_t) - V(s_t)$ is the estimated advantage value at time step t . ϵ is a hyperparameter indicating how much $r_t(\theta)$ can deviate from 1. By taking the minimum of the two terms, the policy is updated within a certain range in each iteration to achieve stable and efficient training.

2) *SAC*: SAC is a maximum entropy reinforcement learning method that maximizes the cumulated reward as well as policy entropy. The loss function of SAC can be expressed as:

$$L(\theta) = E_{s_t \sim D} [\alpha \mathcal{H}(\pi(\cdot|s_t)) - Q(s_t, a_t)]. \quad (4)$$

$\mathcal{H}(\pi(\cdot|s_t)) = -\log \pi_\theta(a_t|s_t)$ is the augmented entropy term and is scaled with a temperature parameter α . With the entropy regularization, SAC encourages the agent to keep a diverse policy and explore different strategies.

B. Reeds-Shepp curve

RS curve is designed to generate the shortest path that links two positions with the minimal steering radius of the vehicle and straight lines. It is mathematically proved that the shortest path belongs to 48 types of curves and can be represented by one of the following 9 expressions:

$$\begin{aligned} & C|C|C, CC|C, CSC, CC_u|C_uC, C|C_uC_u|C, \\ & C|C_{\pi/2}SC, C|C_{\pi/2}SC_{\pi/2}|C, C|C|C, CSC_{\pi/2}|C. \end{aligned} \quad (5)$$

Here, C represents an arc segment with left or right steering, and S represents a straight-line segment. $|$ means the path segment after it uses an opposite direction compared to the one before it. $C_{\pi/2}$ refers to a circular arc in which the central angle is fixed at $\pi/2$, and the arcs noted C_u in one formula share the same central angle u .

When calculating the RS curve, the path scale is initially normalized based on the vehicle's minimal turning radius r_{min} . Subsequently, the lengths of all segments for each type of path are determined using the given scaled starting point $p_0 = (x_0/r_{min}, y_0/r_{min}, \theta_0)$, ending point $p_T = (x_T/r_{min}, y_T/r_{min}, \theta_T)$, and geometric constraints specified by the expression 5. The total length of each path is obtained by summing the lengths of all segments, and the curve with the shortest total length is then selected as the optimal RS curve. The path waypoints $P = \{p_0, p_1, \dots, p_T\}$ along the entire curve can be obtained through interpolation based on the lengths and types of each curve segment. Additionally, the vehicle's steering angle at each waypoint can be calculated using the vehicle model.

IV. METHODOLOGY

A. Overview of architecture

The overall reinforcement learning-based path planning framework and network structure are shown in Figure 1. To enhance training efficiency, we employ a hybrid policy reinforcement learning approach. Our proposed HOPE combines the learnable policy from original reinforcement learning with a rule-based policy derived from the RS curve. In each step, the agent outputs the action, the single-step path planning result, based on the current state given by the environment. The action is then adjusted using the action mask mechanism before interacting with the environment. We employ four forms of network input as state representation, including information about the distance to obstacles, target parking space, drivable action space, and historical trajectory, encoded in either vectors or images. A transformer-based structure with learnable view encoding is designed to fuse the inputs and get the outputs in the actor and critic network [35]. We also utilize the auto-encoder structure to pre-train the image encoder. More details of our network structure and reward function are discussed in the appendix. The pseudo-code of our method is shown in Algorithm 1.

Algorithm 1 The training process of HOPE

```

Initialize the simulation environment E, the agent policy  $\pi_\theta$ ,
the value network  $V_\psi$  and the Q network  $Q_\phi$ , the hybrid
policy  $\pi_h$ , the replay buffer  $D$ 
for  $k = 0, 1, 2, \dots$  do
  Reset the environment:  $t \leftarrow 0, s_t, terminate \leftarrow E$ 
  while  $terminate$  is False:
    Choose action with the hybrid policy  $a_t = \pi_h(s_t)$ 
    Get the masked action  $\hat{a}_t$  using Equation 14, 15
    Interact with E:  $s_{t+1}, r_t, terminate = E(\hat{a}_t)$ 
    Add to  $D$ :  $D = D \cup (s_t, \hat{a}_t, r_t, s_{t+1}, terminate)$ 
    if update condition reached then
      (PPO) Update  $\theta, \psi$  using Equation. 3, 6
      (SAC) Update  $\theta, \phi$  using Equation. 6, 8
    end if
     $t \leftarrow t + 1$ 
  end while
end for

```

B. Hybrid policy

To improve the exploring and training efficiency, we combine the RL policy π_θ and the derived RS policy π_{RS} to facilitate the planning process. The hybrid process at timestamp t can be expressed as a function $h_t : \mathcal{A} \times \mathcal{A} \rightarrow \mathcal{A}$ that maps the actions $a_t \sim \pi_\theta(\cdot|s_t)$ from RL policy and $a'_t \sim \pi_{RS}(\cdot|s_t)$ from RS policy to the hybridized action $\tilde{a}_t = h_t(a_t, a'_t) \sim \pi_h(\cdot|s_t)$. Such an action hybrid process can be regarded as the procedure of making a suitable choice between two actions. Specifically, it activates the rule-based policy at certain timestamps in addition to the reinforcement learning policy, thereby enhancing the robustness of the overall algorithm.

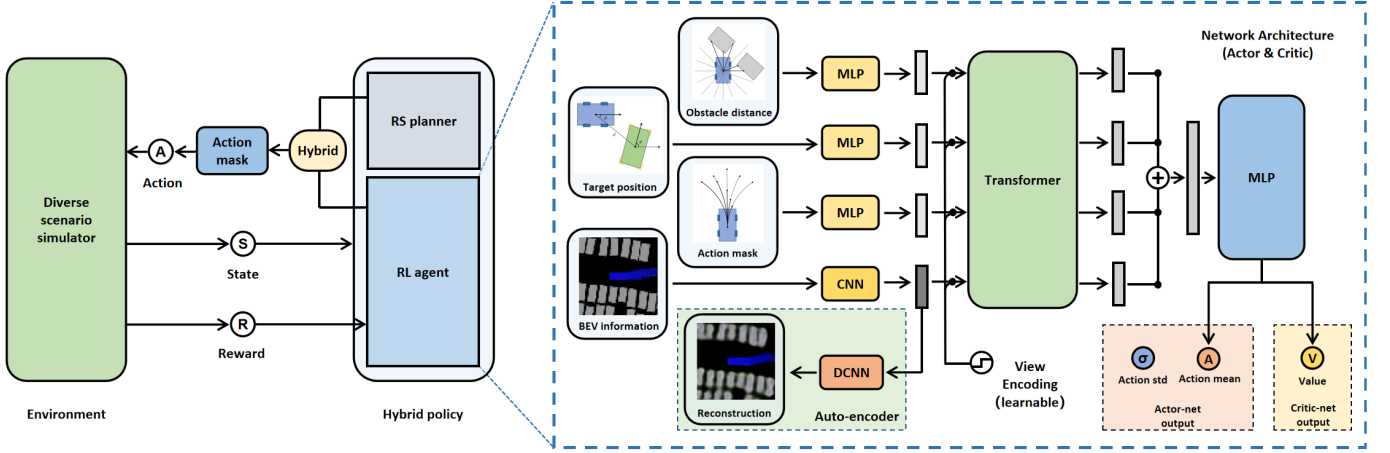


Fig. 1: The overall structure of the proposed method, including the interaction loop with the simulator (left) and the network architecture (right).

1) *Rule-based policy from Reeds-Shepp curve*: The nine expressions in Equation 5 represent 48 types of curves that give the shortest path in free space. However, in the presence of obstacles, the shortest RS curve may not be feasible. To implement the RS method in the parking scenario, we make two modifications in practice:

- We calculated the shortest K curves and verified their feasibility in ascending order of length. The shortest collision-free path is selected to calculate the planning action using the vehicle model.
- We add the computation of the paths in expression $S()C()S$ as these paths, though strictly suboptimal in the absence of obstacles, may be feasible when obstacles are considered. Both real-world parking experience and experiments suggest this is effective for vertical parking.

2) *Exploring and learning with RS policy*: During training, the agent explores and interacts with the environment using the hybridized action \tilde{a}_t rather than raw action a_t . This choice also affects the updates on the policy π_θ and Q function or value function. For the Bellman equation in Equation 2, since the states and actions are obtained with the hybrid policy π_h , the update on the parameter V_ψ and Q_ϕ can be written as:

$$J_V(\psi) = E_{s_t \sim D_{\pi_h}} \left[\frac{1}{2} (V_\psi(s_t) - E_{\tilde{a}_t \sim \pi_h} [Q_\phi(s_t, \tilde{a}_t)])^2 \right]$$

$$J_Q(\phi) = E_{(s_t, \tilde{a}_t) \sim D_{\pi_h}} \left[\frac{1}{2} (Q_\phi(s_t, \tilde{a}_t) - r(s_t, \tilde{a}_t) - \gamma E_{s_{t+1} \sim \rho_{\pi_h}} [V_\psi(s_{t+1})])^2 \right]. \quad (6)$$

Therefore, the update process shown in Equation 6 has the same convergency as Equation 2. For policy updates in PPO, the probability ratio $r_t(\theta)$ in Equation 3 can be rewritten as:

$$r_t(\theta) = \frac{\pi_\theta(a_t|s_t)}{\pi_{\theta_{old}}(\tilde{a}_t|s_t)}, \quad \tilde{a}_t = h(a_t, a'_t). \quad (7)$$

The ratio clipping operation prevents excessive gradient updates caused by a significant KL divergence between π_θ and

π_h . Meanwhile, Equation 4 in SAC can be rewritten as:

$$J_\pi(\theta) = E_{s_t \sim D_{\pi_h}} [\log \pi_\theta(a_t|s_t) - Q_\phi(s_t, a_t)]. \quad (8)$$

Generally, gradients on the Q function and value function are modified by using the data collected by π_h instead of π_θ , since they are now estimations on distribution ρ_{π_h} . We still update the original RL policy π_θ as shown in Equation 7 and 8, which indicates that the hybrid policy π_h , as well as the RL policy π_θ , are optimized. Thus, better performance can be only achieved when $Q_{\pi_h} \geq Q_{\pi_\theta}$ and $V_{\pi_h} \geq V_{\pi_\theta}$. In practice, the RS policy is activated only when: 1) the distance from the vehicle's position to the target position is smaller than a threshold d_{rs} , and 2) there exists a collision-free RS curve from the vehicle's position to the target position. By the hybrid policy approach, during the initial phases of the learning process when the agent is not well-trained, the RS method serves as an alternative strategy to offer additional positive examples for updates. The agent can thus learn how to adjust the vehicle's pose to explore feasible parking routes.

C. Action mask

In some discrete-space reinforcement learning tasks, employing action masks to filter out invalid actions can enhance training efficiency [36]. However, in path planning tasks, the computation of an action mask, which includes collision detection for all feasible actions of the agent vehicle across diverse state spaces, is computationally expensive. Here, we present a method for calculating and utilizing the action mask to enhance the training efficiency of reinforcement learning in path-planning tasks. Specifically, we use $Collide(s_t)$ to denote the event whether the vehicle at state s_t collides with obstacles. The action mask provides information about the largest safe step velocity v^* at any given steering angle δ :

$$v^* = \max_v \{Collide(s_{t+1}) = False\}, \quad (9)$$

where s_{t+1} is the new state after executing action $a = (v, \delta)$ at state s_t . By using v^* to constraint the raw speed v output by the actor net, we can find a collision-free new state using

the masked action. Although calculating this maximum step size for a given action is always feasible, we need to compute the action mask before obtaining the final action and use it to influence the agent's planning. This implies the need to calculate the collision-free v for all given angles.

1) *Efficient estimation of action mask*: We first introduce a vectorized obstacle distance representation l_t at timestamp t , where the i^{th} element $l_t[i]$ is the nearest obstacle distance at angle $\omega_i = i \cdot \Delta\omega$ in the ego coordinate and $\Delta\omega$ is the angular resolution. Consider the envelope area $S_{\mathcal{E}}(\delta_j, v\Delta t)$ covered by the vehicle traveling with a steering angle δ_j and step size $v\Delta t$. Let $\mathcal{E}_{ij}(v)$ denote the distance from the envelope boundary to the origin in the ego vehicle's coordinate system at the i^{th} angle ω_i :

$$\mathcal{E}_{ij}(v) = \max_e \{ \|e\|_2 \mid e = (x, y) \in S_{\mathcal{E}}(\delta_j, v\Delta t), x \sin(\omega_i) = y \cos(\omega_i) \}. \quad (10)$$

The collision constraint can then be expressed as $\mathcal{E}_{ij}(v) \leq l_t[i]$. Then, the action mask calculation is equivalent to the following problem by introducing a variable l :

$$\min l_{ij}; \text{ s. t. } l_{ij} = \mathcal{E}_{ij}(v), l_{ij} \leq l_t[i]. \quad (11)$$

While solving for the optimal l_{ij} is equivalent to obtaining the maximum velocity $v_{ij}^* = \mathcal{E}_{ij}^{-1}(l_t[i])$ considering only obstacle point at i^{th} angle ω_i and vehicle steering angle δ_j , in practice, calculating all envelope distances corresponding to each i and j in each interaction is computationally expensive, and the inverse of \mathcal{E} may not always exist. To deal with this issue, we propose the pre-calculation of the anchoring distance \hat{l}_{ij} for K discretized velocities:

$$\hat{l}_{ij}[k] = \mathcal{E}_{ij}(\hat{v}[k]), \hat{v}[k] = v_{max} \frac{k}{K}, k = 0, 1, \dots, K. \quad (12)$$

Then, we can obtain the upper and lower bounds of the masked velocity v_j^* considering all obstacle points at steering angle δ_j :

$$\begin{aligned} \hat{v}[k_j^*] &\leq v_j^* < \hat{v}[k_j^* + 1], \\ k_j^* &= \min_i \max \{ k : l_t[i] - \hat{l}_{ij}[k] > 0 \}. \end{aligned} \quad (13)$$

We take $v_j^* = \hat{v}[k_j^*]$ as a conservative estimation of max step velocity, and all actions at discretized angle δ_j are calculated in a vectorized manner at once. Since the anchoring distance \hat{l}_{ij} is independent of information of obstacles at timestamp t , a matrix of all anchoring distance $\hat{\mathcal{L}}$ can be pre-calculated before the training process starts. This means that in each interaction step, calculating the action mask only requires the comparison between the two matrices, as shown in Equation 13, which simplifies the calculation.

2) *Combine action mask with agent's policy*: The action mask process can be expressed as a function f_{AM} from raw action to masked action:

$$\hat{a}_t = f_{AM}(\pi_h(s_t)) = h(f_{AM}(\pi_\theta(s_t)), \pi_{RS}(s_t)). \quad (14)$$

Here f_{AM} is applied only to π_θ because π_{RS} provides action only when a feasible RS curve exists. The action mask is also utilized to influence the probability distribution of actions. We here use $f_{am} : \mathcal{A} \rightarrow [0, 1]$ to denote the maximum step size calculated by the action mask, where $f_{am}(a) = p$ indicates the

maximum safe step size is $p \cdot v_{max} \Delta t$. Noticed that $f_{am}(a)$ can serve as a prior probability of $Collide(s_{t+1}) = False$ when $a \sim [a_{min}, a_{max}]$, the action mask can be applied on the distribution of actions from raw network output:

$$\log P(a_t | s_t) = \text{SoftMax}(\log(\pi_\theta(a_t | s_t)) + \log f_{am}(a_t)). \quad (15)$$

The SoftMax here is the probability normalization operation, and $\pi_\theta(a_t | s_t)$ in practice we use a gaussian distribution:

$$\log(\pi_\theta(a | s)) = -\frac{(a - a_{mean})^2}{2a_{std}^2} - \log(\sqrt{2\pi}a_{std}), \quad (16)$$

where a_{mean} is obtained by actor network using input s and a_{std} is a learnable parameter, as shown in Figure 1. Equation 15 shows that the action mask can adjust the probability distribution of actions and avoid invalid actions by taking $f_{am}(a_t) = 0$. We also utilize the post-process in Equation 14 to clip the velocity into a collision-free range in practice.

V. EXPERIMENT

A. scenario difficulty ranking

To better train and evaluate our approach, we rank the difficulty for parking scenarios into normal, complex, and extreme levels based on existing standards *ISO 20900* and *GB/T 41630-2022* [37, 38]. Generally, a parking space is defined by two boundary parking vehicles (or boundary obstacles) positioned on the two sides aligned along the curb-side edge of the road, as shown in Figure 2. The boundaries define the parking space's length L_{park} and width W_{park} . Other obstacles should be placed at least D_{obst} away from the parking spots. We denote the parking vehicle's width as W , length as L , and the distance from the start to the target position as D_{park} . Table I shows the categorization based on the above parameters. Since parallel parking is more challenging than vertical parking in practice, we introduce an extreme difficulty level for it. Besides, we rank the scenarios that $D_{park} > 15.0$ the complex scenario. Note that we do not specify the initial orientation or position of the vehicle, meaning the starting conditions for the vehicle can be any collision-free configuration, which adds to the difficulty and diversity of scenarios.

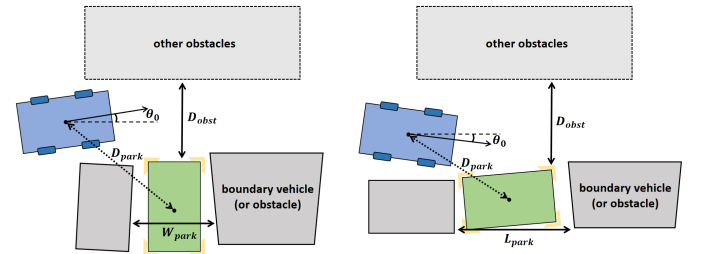


Fig. 2: The description for ranking parameters in vertical parking (left) and parallel parking (right).

Based on the difficulty ranking method, scenarios can be generated and categorized using the pre-defined parameters. In our work, the scenarios are derived from two components:

- Random generation using simulator: As shown in Figure 2, obstacles and the parking spot in a scenario can be represented by multiple randomized parameters. Obstacles

TABLE I: Parking scenario difficulty

| Difficulty | Parallel | Vertical |
|------------|--|--|
| Normal | P(N): $D_{obst} > 4.5$ $L_{park} > \max(L + 1.0, 1.25L)$ | V(N): $D_{obst} > 7.0$ $W_{park} > W + 0.85$ |
| Complex | P(C): $D_{obst} > 4.0$ $L_{park} > \max(L + 0.9, 1.2L)$ | V(C): $D_{obst} > 6.0$ $W_{park} > W + 0.4$ |
| Extreme | P(E): $D_{obst} > 3.5$ $L_{park} > \max(L + 0.6, 1.1L)$ | / |

V: vertical, P: parallel. N, C, and E in the bracket indicate the parking scenario difficulty, i.e., normal, complex, and extreme. unit: meter

may include other stationary vehicles or irregular polygonal obstacles. We randomly set the initial orientation of the start with a Gaussian distribution with $mean(\theta_0) = 0$ and $std(\theta_0) = \pi/6$, and the initial position can be anywhere without collision between parking spots and other obstacles.

- Real-world scenario dataset: We utilize the Dragon Lake Parking (DLP) dataset to construct the DLP scenarios in our simulator [39]. This dataset is constructed from 3.5 hours of video data collected by a drone in a large parking lot, covering an area with about 400 parking spots and 5188 vehicles. While the original dataset was designed for intention and motion prediction tasks, we filtered out non-parking trajectories and dynamic interfering vehicles to obtain 253 static parking scenarios. The starting positions in these parking scenarios are randomly initialized along the recorded paths of the vehicles. These scenarios can be categorized into vertical parking with normal and complex difficulty levels.

B. Implement details

We conducted experiments in Tactics2D, an open-source simulator for driving decision-making [40]. This simulator provides sensor simulations, including lidar and bird's-eye view. In each episode, the simulator independently and randomly initializes the parallel or vertical parking scenarios of three difficulty levels generated by the simulator or from the DLP dataset. Before the episode terminates, the simulator continually updates the vehicle state, calculates the reward, and returns it to the agent after the agent chooses an action. We conducted 100,000 episodes of training and tested 2,000 trials in each scenario category. Details about hyperparameters for algorithm and simulation are listed in Table VII in the appendix.

C. Results

1) *Comaparion with baselines:* We compare the proposed method with the following baselines:

- RS method [7]: The RS method is a classical geometric-based approach that calculates possible path types to obtain feasible routes. In our experiments, we enhance the original RS method by utilizing all calculated paths instead of only the shortest one.
- Hybrid A* [15]: Hybrid A* is a search-based planning method incorporating heuristics considering obstacles and vehicle's non-holonomic constraints during node search. This method is widely applied in various planning tasks in the autonomous driving domain.

- Reinforcement learning baselines: When applying reinforcement learning methods to a specific task, a common practice is to establish a correspondence between the task elements and reinforcement learning components, using a deep network for function approximation. We explored this naive approach in our work, and experiments revealed that both PPO and SAC, in this manner, perform poorly in our parking path planning task.

TABLE II: Planning success rate in different scenarios

| Algorithms | V(N) | P(N) | V(C) | P(C) | P(E) | D(N) | D(C) |
|------------|--------------|-------------|--------------|-------------|-------------|-------------|-------------|
| RS | 36.9 | 10.4 | 30.4 | 1.5 | 0.3 | 4.0 | 0.1 |
| Hybrid A* | 99.4 | 90.2 | 99.2 | 60.2 | 16.8 | 98.7 | 85.6 |
| PPO | 93.2 | 74.2 | 82.9 | 69.0 | 58.4 | 65.2 | 34.2 |
| SAC | 93.8 | 33.7 | 92.9 | 29.6 | 18.9 | 33.3 | 32.7 |
| HOPE(PPO) | 100.0 | 99.4 | 99.8 | 97.5 | 94.2 | 99.5 | 97.6 |
| HOPE(SAC) | 100.0 | 99.7 | 100.0 | 99.4 | 97.5 | 99.4 | 98.0 |

D: DLP scenarios. unit: percentage

Table II presents the planning success rates of these methods across different scene types and difficulty levels. We have separately listed the results for DLP scenarios since they originate from real-world parking environments. As shown in the table, a direct implementation of the RS method fails to provide a feasible path in most cases. Hybrid A* achieves a success rate of over 90% in both normal scenarios and complex vertical parking cases. However, as the scene difficulty increases, its planning success rate significantly declines. In the extreme parallel parking scenarios, the most narrow cases, its success rate is only 16.8%. The reinforcement learning baselines perform better than the rule-based RS method but fail to surpass the Hybrid A*. Their low success rates in several scenarios demonstrate that achieving good performance through overfitting in a few cases does not necessarily guarantee the trained agent's generalization capability. In contrast, our proposed HOPE, no matter based on on-policy PPO or off-policy SAC, outperforms all baselines and reaches a success rate of over 99.4% in all normal scenarios and over 94% in all scenarios. Figure 3 shows the reward and success rate curves in the training process. By combining the RL agent and the RS policy, the proposed method significantly improves training efficiency and success rate over the naive RL method.

2) *Further comparison with Hybrid A*:* As the Hybrid A* is a widely used method to this day, we further compare our approach with it through specific case studies. As shown in Figure 4, while both two methods can mask successful path planning in some cases, our method is capable of providing more concise and reasonable planning results, such as in

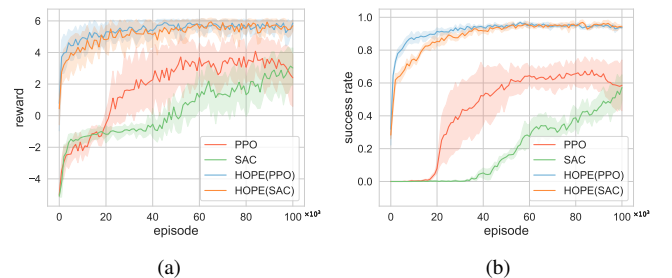


Fig. 3: The episode reward curves (a) and success rate (b)

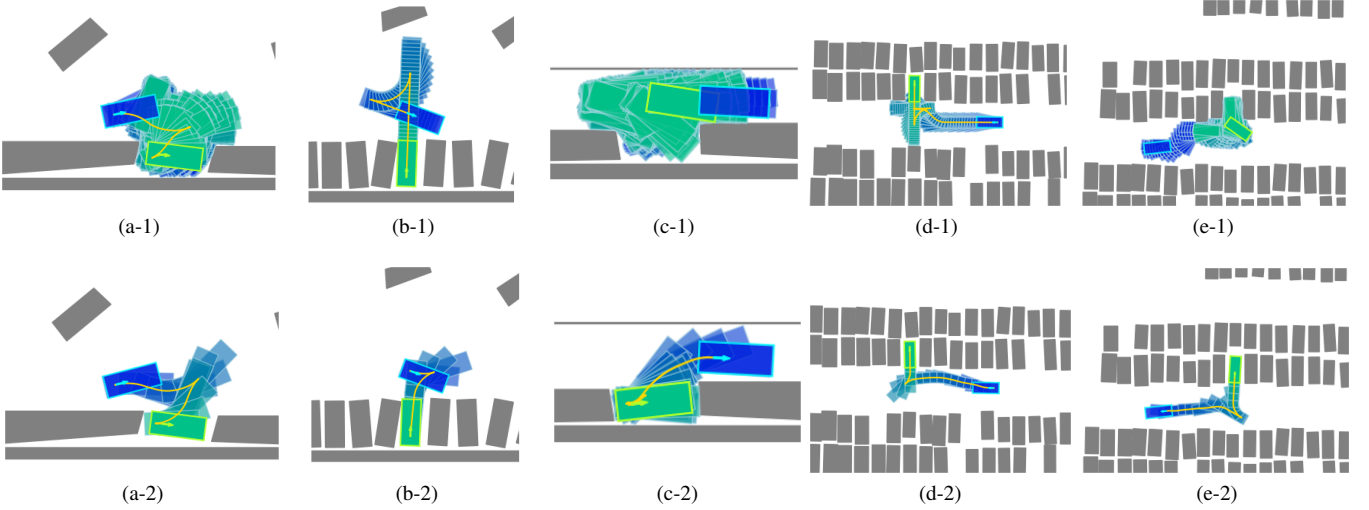


Fig. 4: The visualization of the planning process and results of the Hybrid A* (a-1)-(e-1) and the proposed HOPE (a-2)-(e-2). In the normal parallel parking case shown in (a), both methods provide concise path planning results. In the vertical parking scenario shown in (b) and the normal dlp scenario in (d), although both methods succeed in planning, our approach yields more reasonable results. Meanwhile, in the narrow parallel parking scenario (c) and the scenario requiring parking with the front of the vehicle facing inward (e), the Hybrid A* algorithm fails to plan, while our approach succeeds.

Figure 4 (b) and (d). As the parking space in the scene becomes narrow, Hybrid A* struggles to explore a feasible path. In contrast, our method, through training, achieves the ability to maneuver within tight parking spaces and overcome local optima situations, as shown in Figure 4 (c) and (e).

3) *Computational consumption*: The average time consumption for a single-step prediction is 8.5 ms and can be broken down as follows: 2.7 ms for a single-step network forwarding, 2.8 ms for action mask calculation, and 3.0 ms for RS curve calculation. The simulator takes 8.3 ms each step for kinematics simulation and other information rendering. The total time required to generate a complete planning result, including algorithmic computation and simulator simulation overhead, is shown in Table III.

TABLE III: Time cost of complete path generation on average

| Alg. | V(N) | P(N) | V(C) | P(C) | P(E) | D(N) | D(C) |
|-----------|-------|-------|-------|-------|-------|-------|-------|
| HOPE(PPO) | 314.6 | 451.6 | 369.1 | 549.8 | 891.4 | 433.0 | 699.0 |
| HOPE(SAC) | 304.4 | 372.3 | 328.0 | 476.6 | 638.4 | 464.8 | 633.2 |

unit: microsecond(ms)

D. Ablation studies

1) *Hybrid policy with RS-curve*: We designed experiments to investigate how the use of the RS method influences the performance of the hybrid policy. A hyperparameter in the hybrid strategy is the threshold distance d_{rs} . The RS policy is considered only when the vehicle is closer to the target position than d_{rs} . The results show that even reducing d_{rs} to 1 m has less than a 5% impact on the success rate while increasing d_{rs} does not lead to a significant improvement. This result indicates that while RS curves assist in training the hybrid policy, the reinforcement learning agent does not overly rely on the RS method, allowing it to outperform rule-based approaches.

Besides, while the original RS method only utilizes the shortest path, the shortest K paths are considered in the hybrid

TABLE IV: Experiment on threshold distance for RS curve

| Alg. | d_{rs} | V(N) | P(N) | V(C) | P(C) | P(E) | D(N) | D(C) |
|------------|----------|-------|------|-------|------|------|------|------|
| HOPE (PPO) | 1 | 99.2 | 97.4 | 95.4 | 95.0 | 92.6 | 97.1 | 95.0 |
| | 5 | 99.6 | 98.7 | 97.6 | 96.1 | 93.2 | 99.5 | 96.7 |
| | 10 | 100.0 | 99.4 | 99.8 | 97.5 | 94.2 | 99.5 | 97.6 |
| | 15 | 100.0 | 99.3 | 99.8 | 96.6 | 94.2 | 99.9 | 98.4 |
| HOPE (SAC) | 1 | 99.8 | 97.8 | 99.4 | 98.9 | 97.8 | 95.8 | 89.1 |
| | 5 | 100.0 | 98.0 | 99.8 | 99.2 | 97.7 | 99.4 | 97.3 |
| | 10 | 100.0 | 99.7 | 100.0 | 99.4 | 97.5 | 99.4 | 98.0 |
| | 15 | 100.0 | 99.4 | 100.0 | 99.0 | 98.2 | 99.0 | 98.1 |

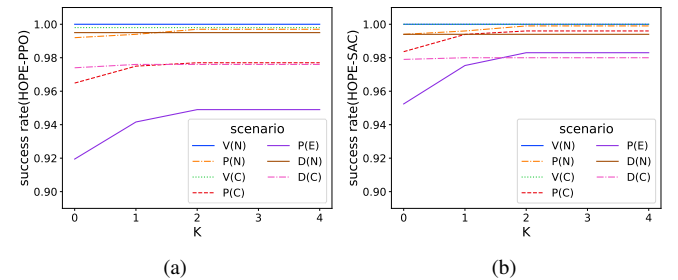


Fig. 5: Success rate using the shortest K RS curves.

policy. In practice, we choose $K = 2$ to avoid redundant computations. At this point, the algorithm's performance has nearly saturated, as shown in Figure 5.

2) *Other proposed modules*: More ablation experiment results are presented in Table V. In the absence of the action mask mechanism, the success rate declines by more than 20% in complex parallel parking scenarios and 30% in extreme scenarios. This significant drop in performance indicates that utilizing an action mask to influence and constrain the agent's action is crucial for training effectiveness. Besides, replacing the transformer with a multi-layer perceptron leads to a decline of more than 10% in several scenarios, demonstrating the importance of multi-modal information fusion. Excluding the action mask or bird's-eye view (BEV) images as inputs to the

neural network also impacts the agent’s performance. Using the auto-encoder to pre-train the image encoder can enhance the training for the PPO-based agent but has a relatively minor impact on the SAC-based agent.

TABLE V: Ablation experiment

| Experiments | V(N) | P(N) | V(C) | P(C) | P(E) | D(N) | D(C) |
|-------------|-------|------|-------|------|------|------|------|
| HOPE(PPO) | 100.0 | 99.4 | 99.8 | 97.5 | 94.2 | 99.5 | 97.6 |
| -AMP | 96.9 | 94.7 | 96.0 | 70.1 | 62.4 | 92.8 | 75.4 |
| MLP | 99.8 | 98.5 | 99.7 | 93.3 | 82.8 | 99.4 | 92.1 |
| -AMI | 99.6 | 99.0 | 98.1 | 97.3 | 91.0 | 98.8 | 94.4 |
| -BEV | 100.0 | 98.8 | 99.9 | 96.1 | 92.8 | 99.4 | 93.5 |
| -AE | 99.9 | 98.2 | 99.5 | 95.4 | 86.2 | 97.0 | 85.7 |
| HOPE(SAC) | 100.0 | 99.7 | 100.0 | 99.4 | 97.5 | 99.4 | 98.0 |
| -AMP | 96.5 | 49.1 | 96.3 | 36.5 | 23.4 | 78.2 | 57.2 |
| MLP | 99.8 | 90.6 | 98.8 | 82.3 | 72.1 | 97.8 | 87.9 |
| -AMI | 99.9 | 96.4 | 98.7 | 91.9 | 84.9 | 97.2 | 92.3 |
| -BEV | 99.8 | 97.8 | 98.7 | 97.9 | 97.6 | 98.1 | 96.5 |
| -AE | 100.0 | 99.8 | 100.0 | 99.0 | 96.7 | 99.7 | 99.0 |

-AMP: omit the action mask mechanism in post-processing. MLP: use MLP instead of transformer as the network backbone. -AMI: exclude the use of the action mask in network input. -BEV: exclude the BEV image in network input. -AE: not employ auto-encoder to pre-train the image encoder.

3) *Scenario difficulty*: We also examined the impact of restricting the training scenario difficulty on the agent’s performance. As shown in Table VI, training solely on normal cases leads to a 20% to 30% decline in success rate in extreme scenarios, even with the help of the RS policy and action mask mechanism. Generalization capability under all difficulties can only be achieved when the training scenarios are sufficiently complex and diverse, which also underscores the importance of ranking difficulty in scenario taxonomy.

TABLE VI: Experiments on training scenario difficulty

| difficulty | V(N) | P(N) | V(C) | P(C) | P(E) | D(N) | D(C) |
|------------|-------|-------|-------|-------|------|------|------|
| HOPE (PPO) | N | 100.0 | 98.4 | 99.8 | 89.5 | 64.6 | 99.8 |
| +C | 99.9 | 98.5 | 99.9 | 94.8 | 76.1 | 99.9 | 98.1 |
| +E | 100.0 | 99.4 | 99.8 | 97.5 | 94.2 | 99.5 | 97.6 |
| HOPE (SAC) | N | 100.0 | 97.6 | 100.0 | 91.1 | 77.6 | 98.4 |
| +C | 100.0 | 98.3 | 100.0 | 91.5 | 80.0 | 99.7 | 95.4 |
| +E | 100.0 | 99.7 | 100.0 | 99.4 | 97.5 | 99.4 | 98.0 |

N: use only normal cases in training. +C: use normal and complex cases. +E: use cases of all difficulty levels.

VI. CONCLUSION AND FUTURE WORK

In this paper, we proposed a reinforcement learning-based path planning method in diverse parking scenarios with static obstacles. Instead of directly training the parking agent with existing RL methods, we introduced a hybrid policy that integrates the RS curve and PPO as well as SAC. To enhance the training efficiency and performance of reinforcement learning agents, we introduce a method to calculate and implement the action mask mechanism in the task of parking path planning. A transformer-based network structure is utilized to fuse information about obstacles and target parking spots from different inputs and output the planning actions.

To better train and evaluate the proposed method, we introduce a difficulty ranking approach for parking scenarios. The difficulty ranking standard categorizes scenarios into normal, complex, and extreme based on obstacles and parking space conditions. We utilized a simulator and a real-world parking lot dataset to construct training and testing scenarios.

Comparisons were made against the Hybrid A* algorithm and the naive PPO and SAC. Comprehensive experiments were designed to illustrate the effectiveness of the proposed method. The results indicate that our approach outperforms the Hybrid A* algorithm in planning success rates across all types of scenarios, particularly in complex and extreme situations. Compared to the typical approach of directly using reinforcement learning for training, our proposed method combines the advantages of both rule-based and learning-based methods, resulting in an effectively trained planner with generalization capabilities across different scenarios.

This paper shows that the learning-based approach can serve as a promising tool in dealing with complex and diverse parking scenarios. Our work will be open-sourced to support the following research. We are planning to implement our algorithm within an automated parking system in an infrastructure-based indoor automated parking task. The proposed HOPE serves as a potential planner to deal with the intricate scenarios where the rule-based methods fail to plan a feasible path. Besides, since only static scenarios are considered in our work, more efforts could be made to apply the learning-based method in parking scenarios with dynamic obstacles in the future.

REFERENCES

- [1] Y. Song and C. Liao, “Analysis and review of state-of-the-art automatic parking assist system,” in *2016 IEEE International Conference on Vehicular Electronics and Safety (ICVES)*. IEEE, 2016, pp. 1–6.
- [2] W. Wang, Y. Song, J. Zhang, and H. Deng, “Automatic parking of vehicles: A review of literatures,” *International Journal of Automotive Technology*, vol. 15, pp. 967–978, 2014.
- [3] A. Likmeta, A. M. Metelli, A. Tirinzoni, R. Giol, M. Restelli, and D. Romano, “Combining reinforcement learning with rule-based controllers for transparent and general decision-making in autonomous driving,” *Robotics and Autonomous Systems*, vol. 131, p. 103568, 2020.
- [4] S. Teng, X. Hu, P. Deng, B. Li, Y. Li, Y. Ai, D. Yang, L. Li, Z. Xuanyuan, F. Zhu *et al.*, “Motion planning for autonomous driving: The state of the art and future perspectives,” *IEEE Transactions on Intelligent Vehicles*, 2023.
- [5] B. R. Kiran, I. Sobh, V. Talpaert, P. Mannion, A. A. Al Sallab, S. Yogamani, and P. Pérez, “Deep reinforcement learning for autonomous driving: A survey,” *IEEE Transactions on Intelligent Transportation Systems*, vol. 23, no. 6, pp. 4909–4926, 2021.
- [6] S. Grigorescu, B. Tranea, T. Cocias, and G. Macesanu, “A survey of deep learning techniques for autonomous driving,” *Journal of Field Robotics*, vol. 37, no. 3, pp. 362–386, 2020.
- [7] J. Reeds and L. Shepp, “Optimal paths for a car that goes both forwards and backwards,” *Pacific journal of mathematics*, vol. 145, no. 2, pp. 367–393, 1990.
- [8] A. Vaswani, N. Shazeer, N. Parmar, J. Uszkoreit, L. Jones, A. N. Gomez, Ł. Kaiser, and I. Polosukhin,

- “Attention is all you need,” *Advances in neural information processing systems*, vol. 30, 2017.
- [9] B. Li, T. Acarman, Y. Zhang, Y. Ouyang, C. Yaman, Q. Kong, X. Zhong, and X. Peng, “Optimization-based trajectory planning for autonomous parking with irregularly placed obstacles: A lightweight iterative framework,” *IEEE Transactions on Intelligent Transportation Systems*, vol. 23, no. 8, pp. 11 970–11 981, 2021.
 - [10] Z. Liang, G. Zheng, and J. Li, “Automatic parking path optimization based on bezier curve fitting,” in *2012 IEEE International Conference on Automation and Logistics*. IEEE, 2012, pp. 583–587.
 - [11] H. Vorobieva, S. Glaser, N. Minoiu-Enache, and S. Mammar, “Automatic parallel parking with geometric continuous-curvature path planning,” in *2014 IEEE Intelligent Vehicles Symposium Proceedings*. IEEE, 2014, pp. 465–471.
 - [12] L. E. Dubins, “On curves of minimal length with a constraint on average curvature, and with prescribed initial and terminal positions and tangents,” *American Journal of mathematics*, vol. 79, no. 3, pp. 497–516, 1957.
 - [13] X. Du and K. K. Tan, “Autonomous reverse parking system based on robust path generation and improved sliding mode control,” *IEEE Transactions on Intelligent Transportation Systems*, vol. 16, no. 3, pp. 1225–1237, 2014.
 - [14] J. M. Kim, K. I. Lim, and J. H. Kim, “Auto parking path planning system using modified reeds-shepp curve algorithm,” in *2014 11th International Conference on Ubiquitous Robots and Ambient Intelligence (URAI)*. IEEE, 2014, pp. 311–315.
 - [15] D. Dolgov, S. Thrun, M. Montemerlo, and J. Diebel, “Path planning for autonomous vehicles in unknown semi-structured environments,” *The international journal of robotics research*, vol. 29, no. 5, pp. 485–501, 2010.
 - [16] S. Sedighi, D.-V. Nguyen, and K.-D. Kuhnert, “Guided hybrid a-star path planning algorithm for valet parking applications,” in *2019 5th international conference on control, automation and robotics (ICCAR)*. IEEE, 2019, pp. 570–575.
 - [17] W. Sheng, B. Li, and X. Zhong, “Autonomous parking trajectory planning with tiny passages: a combination of multistage hybrid a-star algorithm and numerical optimal control,” *IEEE Access*, vol. 9, pp. 102 801–102 810, 2021.
 - [18] M. Czubenko, Z. Kowalczyk, and A. Ordys, “Autonomous driver based on an intelligent system of decision-making,” *Cognitive computation*, vol. 7, pp. 569–581, 2015.
 - [19] X. Zhang, A. Liniger, and F. Borrelli, “Optimization-based collision avoidance,” *IEEE Transactions on Control Systems Technology*, vol. 29, no. 3, pp. 972–983, 2020.
 - [20] R. He, J. Zhou, S. Jiang, Y. Wang, J. Tao, S. Song, J. Hu, J. Miao, and Q. Luo, “Tdr-obca: A reliable planner for autonomous driving in free-space environment,” in *2021 American Control Conference (ACC)*. IEEE, 2021, pp. 2927–2934.
 - [21] Z. Han, Y. Wu, T. Li, L. Zhang, L. Pei, L. Xu, C. Li, C. Ma, C. Xu, S. Shen *et al.*, “An efficient spatial-temporal trajectory planner for autonomous vehicles in unstructured environments,” *IEEE Transactions on Intelligent Transportation Systems*, 2023.
 - [22] W. Liu, Z. Li, L. Li, and F.-Y. Wang, “Parking like a human: A direct trajectory planning solution,” *IEEE Transactions on Intelligent Transportation Systems*, vol. 18, no. 12, pp. 3388–3397, 2017.
 - [23] S. Rathour, V. John, M. Nithilan, and S. Mita, “Vision and dead reckoning-based end-to-end parking for autonomous vehicles,” in *2018 IEEE Intelligent Vehicles Symposium (IV)*. IEEE, 2018, pp. 2182–2187.
 - [24] R. Chai, A. Tsourdos, A. Savvaris, S. Chai, Y. Xia, and C. P. Chen, “Design and implementation of deep neural network-based control for automatic parking maneuver process,” *IEEE Transactions on Neural Networks and Learning Systems*, vol. 33, no. 4, pp. 1400–1413, 2020.
 - [25] R. Chai, D. Liu, T. Liu, A. Tsourdos, Y. Xia, and S. Chai, “Deep learning-based trajectory planning and control for autonomous ground vehicle parking maneuver,” *IEEE Transactions on Automation Science and Engineering*, 2022.
 - [26] J. Ho and S. Ermon, “Generative adversarial imitation learning,” *Advances in neural information processing systems*, vol. 29, 2016.
 - [27] S. Song, H. Chen, H. Sun, M. Liu, and T. Xia, “Time-optimized online planning for parallel parking with nonlinear optimization and improved monte carlo tree search,” *IEEE Robotics and Automation Letters*, vol. 7, no. 2, pp. 2226–2233, 2022.
 - [28] V. Mnih, K. Kavukcuoglu, D. Silver, A. A. Rusu, J. Veness, M. G. Bellemare, A. Graves, M. Riedmiller, A. K. Fidjeland, G. Ostrovski *et al.*, “Human-level control through deep reinforcement learning,” *nature*, vol. 518, no. 7540, pp. 529–533, 2015.
 - [29] J. Bernhard, R. Giesemann, K. Esterle, and A. Knoll, “Experience-based heuristic search: Robust motion planning with deep q-learning,” in *2018 21st International conference on intelligent transportation systems (ITSC)*. IEEE, 2018, pp. 3175–3182.
 - [30] Z. Du, Q. Miao, and C. Zong, “Trajectory planning for automated parking systems using deep reinforcement learning,” *International Journal of Automotive Technology*, vol. 21, pp. 881–887, 2020.
 - [31] Z. Yuan, Z. Wang, X. Li, L. Li, and L. Zhang, “Hierarchical trajectory planning for narrow-space automated parking with deep reinforcement learning: A federated learning scheme,” *Sensors*, vol. 23, no. 8, p. 4087, 2023.
 - [32] M. Althoff, M. Koschi, and S. Manzing, “Commonroad: Composible benchmarks for motion planning on roads,” in *2017 IEEE Intelligent Vehicles Symposium (IV)*. IEEE, 2017, pp. 719–726.
 - [33] J. Schulman, F. Wolski, P. Dhariwal, A. Radford, and O. Klimov, “Proximal policy optimization algorithms,” *arXiv preprint arXiv:1707.06347*, 2017.
 - [34] T. Haarnoja, A. Zhou, P. Abbeel, and S. Levine, “Soft

actor-critic: Off-policy maximum entropy deep reinforcement learning with a stochastic actor,” in *International conference on machine learning*. PMLR, 2018, pp. 1861–1870.

- [35] H. Shao, L. Wang, R. Chen, H. Li, and Y. Liu, “Safety-enhanced autonomous driving using interpretable sensor fusion transformer,” in *Conference on Robot Learning*. PMLR, 2023, pp. 726–737.
- [36] S. Huang and S. Ontañón, “A closer look at invalid action masking in policy gradient algorithms,” *arXiv preprint arXiv:2006.14171*, 2020.
- [37] “Intelligent transport systems - partially-automated parking systems (paps) - performance requirements and test procedures,” ISO 20900:2023, 2023.
- [38] “Performance requirements and test methods for intelligent parking assist system,” GB/T 41630-2022, 2022.
- [39] X. Shen, M. Lacayo, N. Guggilla, and F. Borrelli, “Parkpredict+: Multimodal intent and motion prediction for vehicles in parking lots with cnn and transformer,” in *2022 IEEE 25th International Conference on Intelligent Transportation Systems (ITSC)*. IEEE, 2022, pp. 3999–4004.
- [40] Y. Li, S. Zhang, M. Jiang, X. Chen, and M. Yang, “Tactics2d: A multi-agent reinforcement learning environment for driving decision-making,” *arXiv preprint arXiv:2311.11058*, 2023.



Mingyang Jiang received a Bachelor’s degree in engineering from Shanghai Jiao Tong University, Shanghai, China, in 2023. He is working towards a Master’s degree in Control Science and Engineering from Shanghai Jiao Tong University. His main research interests are end-to-end planning, driving decision-making, and reinforcement learning for autonomous vehicles.



Yueyuan LI received a Bachelor’s degree in Electrical and Computer Engineering from the University of Michigan-Shanghai Jiao Tong University Joint Institute, Shanghai, China, in 2020. She is working towards a Ph.D. degree in Control Science and Engineering from Shanghai Jiao Tong University.

Her main fields of interest are the security of the autonomous driving system and driving decision-making. Her current research activities include driving decision-making models, driving simulation, and virtual-to-real model transferring.



inforcement learning, and meta-reinforcement learning for autonomous vehicle decision-making.

Songan Zhang received B.S. and M.S. degrees in automotive engineering from Tsinghua University in 2013 and 2016, respectively. Then, she went to the University of Michigan, Ann Arbor, and got a Ph.D. in mechanical engineering in 2021. After graduation, she worked at Ford Motor Company in the Robotics Research Team as a research scientist. Presently, she is an assistant professor at the Global Institute of Future Technology (GIFT) in Shanghai Jiao Tong University. Her research interests include accelerated evaluation of autonomous vehicles, model-based



Chunxiang WANG received a Ph.D. degree in Mechanical Engineering from Harbin Institute of Technology, China, in 1999. She is currently an associate professor in the Department of Automation at Shanghai Jiao Tong University, Shanghai, China.

She has been working in the field of intelligent vehicles for more than ten years and has participated in several related research projects, such as European CyberC3 project, ITER transfer cask project, etc. Her research interests include autonomous driving, assistant driving, and mobile robots.



Ming YANG received his Master’s and Ph.D. degrees from Tsinghua University, Beijing, China, in 1999 and 2003, respectively. Presently, he holds the position of Distinguished Professor at Shanghai Jiao Tong University, also serving as the Director of the Innovation Center of Intelligent Connected Vehicles. Dr. Yang has been engaged in the research of intelligent vehicles for more than 25 years.

APPENDIX A IMPLEMENTATION OF INFORMATION FUSION TRANSFORMER

In our approach, both vectorized and visual representations are employed to convey state information. These inputs of the network include:

- Obstacle distance(vector-based) l_t : the value of the nearest distance to obstacles at certain angles, as defined in section IV-C1, which is similar to the scan results of a single-line lidar.
- Target position(vector-based) P_{tgt} : P_{tgt} is defined as a 5-elements tuple $(d, \cos(\theta_t), \sin(\theta_t), \cos(\phi_t), \sin(\phi_t))$, includes the information about distance to target parking spot's position d , orientation θ_t , and heading ϕ_t in the ego vehicle's coordinate system.
- Action mask(vector-based) f_{am} : a discretization of action mask that describes the max valid step size at different steering angles, as defined in section IV-C2.
- Bird-eye-view information(image-based) I_{BEV} : a low-resolution depiction of the surrounding obstacle, target parking spot. The historical trajectory of the ego vehicle is rendered using a gradient color scheme. The image size is $H_{img} \cdot W_{img}$.

We employ a multi-layer perceptron model for vector-based input to encode it into a feature token. For image-based input, we use a convolution neural network(CNN) with residual blocks to extract 2D features, which are later flattened to match the dimensions of other tokens. Tokens from different views are then fused in the transformer encoder, and their values are selected as outputs. Finally, an MLP-based network is used to map the concatenation of the values to the target output, namely the action for actor-net or the estimated value for value-net. Moreover, we use an auto-encoder structure to train the encoder in self-supervision. The CNN encoder extracts the features from the original image, and a deconvolutional neural network is used to reconstruct the image from the features. The pre-training data is collected with a naive agent trained initially without image input. The loss function of the auto-encoder using a mean square error can be expressed as:

$$L_{AE} = \|\text{Decoder}(\text{Encoder}(I_{BEV})) - I_{BEV}\|_2^2. \quad (17)$$

APPENDIX B REWARD FUNCTION

A basic reward design involves assigning a positive reward r_{succ} when the goal is completed and a negative penalty r_{fail} when the interaction terminates in failure. Based on this, we design several additional step rewards to encourage the agent to get close to the success state.

1) *Intersection-of-union(IOU) reward*: The IOU area of the vehicle bounding box and the target parking spot is selected as guidance. We denote $\text{IOU}(s_t)$ as the IOU area of vehicle at time step t , and the IOU reward is:

$$r_{\text{IOU}}(t) = \max(\text{IOU}(s_t) - \max_{i \in (0, t-1)} \text{IOU}(s_i), 0). \quad (18)$$

This reward focuses on the increase of the IOU area compared to the largest value reached before and does not penalize it when the vehicle attempts to move out of the parking spot.

2) *Distance reward*: We assign a positive reward to the agent when the vehicle is getting closer to parking spots:

$$r_{\text{dist}}(t) = -\frac{(D(t) - D(0))}{\max(D(0), D_{\min})}. \quad (19)$$

$D(t)$ is the distance from the vehicle to the target position at time step t . D_{\min} is a hyperparameter to avoid too large reward value.

3) *Time consumption penalty*: For each interaction, the agent receives a small negative penalty as the cost of interaction, and this penalty increases over time. We bound the penalized value with \tanh :

$$r_{\text{time}}(t) = -\tanh(t/(10 \cdot T_{\max})). \quad (20)$$

Here T_{\max} is the maximum interaction times in an episode.

4) *Overall reward function*: The above basic rewards and step rewards are linearly combined to form the final reward function:

$$r = w_1 r_{\text{succ}} + w_2 r_{\text{fail}} + w_3 r_{\text{IOU}} + w_4 r_{\text{dist}} + w_5 r_{\text{time}}. \quad (21)$$

In practice, we set $r_{\text{succ}} = 5$, $r_{\text{fail}} = -5$, $w_1 = w_2 = w_3 = 1$, $w_4 = 0.5$ and $w_5 = 0.1$.

APPENDIX C HYPERPARAMETERS

The key parameters for the algorithm and simulation are listed in Table VII. Besides, the training process was conducted on an NVIDIA GeForce RTX 3090 GPU and AMD EPYC 7542 CPU, and evaluation was performed on an NVIDIA GeForce RTX 3060 GPU and Intel i7-11800H CPU.

TABLE VII: Parameters in simulation and algorithm

| Parameter | Description | Value |
|----------------------------------|--|--------------|
| lr_{actor} | Learning rate for the actor-network | 5e-6 |
| lr_{critic} | Learning rate for the critic-network | 2.5e-5 |
| $ D $ | Replay buffer size | 8192 |
| γ | Discount factor for rewards | 0.98 |
| ϵ | Clipping parameter in PPO | 0.2 |
| d_{rs} | Threshold distance for the RS policy | 10.0 |
| T_{\max} | Maximum interaction times in a episode | 200 |
| n_{MLP} | Number of layers in the input MLP | 2 |
| n_{CNN} | Number of layers in the input CNN | 2 |
| d_{token} | The size of embedded tokens | 128 |
| d_{hidd} | The size of hidden layers | 128 |
| n_{attn} | Number of attention layers | 1 |
| n_{head} | Parameters of multi-head mechanism | 8 |
| n_{out} | Number of layers in the output MLP | 2 |
| $\Delta\omega$ | Simulated lidar angular resolution | $\pi/60$ rad |
| R_{lidar} | Simulated maximum lidar range | 10 m |
| $H_{\text{img}}(W_{\text{img}})$ | BEV image height (width) | 64 px |
| L | Vehicle length | 4.69 m |
| W | Vehicle width | 1.94 m |
| v_{\max} | Maximum velocity | 2.5 m/s |
| δ_{\max} | Maximum steering angle | 0.75 rad |